Desalination 573 (2024) 117209

Contents lists available at ScienceDirect

Desalination

journal homepage: www.elsevier.com/locate/desal

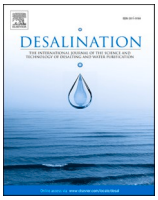

A hybrid process combining ion exchange resin and bipolar membrane electrodialysis for reverse osmosis remineralization

A.A.M. Abusultan [a], J.A. Wood [a], T. Sainio [b], A.J.B. Kemperman [a,*], W.G.J. van der Meer [a,c]

[a] Membrane Science and Technology Cluster, MESA+ Institute for Nanotechnology, Faculty of Science and Technology, University of Twente, P.O. Box 217, NL-7500 AE Enschede, the Netherlands.
[b] LUT University, School of Engineering Science, Department of Separation Science, Mukkulankatu 19, 15210 Lahti, Finland
[c] Oasen N.V., P.O. Box 122, 2800 AC Gouda, the Netherlands

HIGHLIGHTS

- A new remineralization process for RO permeate is proposed.
- The process is based on a combined ion exchange-bipolar membrane hybrid process.
- Cation exchange is used for hardness removal and recovery.
- Bipolar membrane electrodialysis is used for HCl and NaOH production from NaCl.
- Total treatment cost is comparable to conventional remineralization processes.

GRAPHICAL ABSTRACT

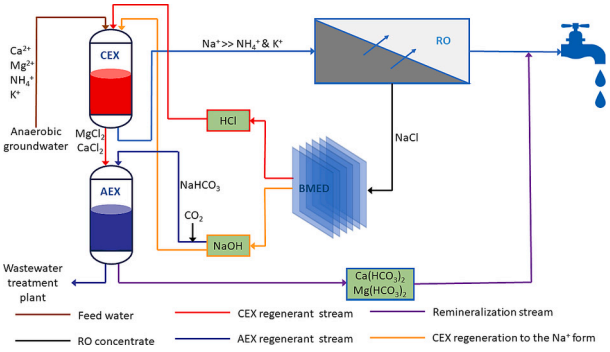

ARTICLE INFO

Keywords:
Ion exchange resin
Ion exchange membrane
Bipolar membrane
Electrodialysis
Reverse osmosis
Remineralization

ABSTRACT

A new reverse osmosis (RO) permeate remineralization process combining ion exchange resin and bipolar membrane electrodialysis (BMED) was developed. Its feasibility for hardness ions recovery and RO permeate remineralization was investigated. The effect of several operation conditions on the efficiency of the combined remineralization process was studied. Highly efficient cation exchange resin loading was achieved at a low flow rate and low feed solution concentration. The recovered calcium purity and yield considerably improved under gradient elution methods in comparison with commonly applied conventional isocratic elution methods using the same eluent quantity. The purity of the produced acid and base using BMED dropped noticeably with increasing feed NaCl concentration, presumably related to decreased permselectivity of the ion-exchange membranes. The drop in the purity of the calcium recovered when eluting the cation exchange resin with BMED-produced HCl in comparison with commercially available acid at 50 % yield was shown not to affect the remineralization process, where a dilution factor could be applied. This study confirmed the technical feasibility of the developed process for RO permeate remineralization. However, its application can be limited by the water source characteristics, the energy-intensive bipolar membrane process, and applied operational conditions, where more investigation is still needed.

* Corresponding author.
E-mail address: a.j.b.kemperman@utwente.nl (A.J.B. Kemperman).

https://doi.org/10.1016/j.desal.2023.117209
Received 8 August 2023; Received in revised form 28 November 2023; Accepted 1 December 2023
Available online 5 December 2023

1. Introduction

Water shortages across the globe due to climate change and increased demand have triggered the need for furthering the development of sustainable and highly efficient water treatment solutions. According to the WHO/UNICEF joint report recently published, around one-fifth of the world's population does not have access to safely managed drinking water services [1]. Water treatment using membrane filtration and in particular reverse osmosis (RO) has emerged as a viable solution for producing clean drinking water. Reverse osmosis (RO) is the most commonly applied membrane filtration process in drinking water applications; it forms more than three-quarters of the total installed and projected desalination capacity [2]. Despite that, reverse osmosis was originally developed to remove salt from seawater but is being used more often to treat fresh/brackish groundwater. RO is advantageous when compared to conventional water treatment methods (including coagulation, sedimentation, sand filtration, activated carbon filtration, disinfection, etc.), since it is capable of removing newly emerging contaminants (such as micropollutants, pharmaceuticals, etc.) [3,4], treating high salinity water, and producing RO permeate with lower bacterial growth potential [5]. Yet, RO application in treating fresh water is still limited, since RO typically must be operated at lower recovery (~80 %), due to the scaling potential induced by divalent ions presence such as calcium carbonate and barium sulphate etc., compared to conventional water treatment methods (~5 % water loss in sand filters backwash cycles) [6–8]. Moreover, a side effect of using RO for water treatment is the production of a relatively concentrated waste stream.

The One Step Reverse Osmosis (OSRO) concept is currently applied in the Netherlands to treat fresh/brackish groundwater with a single step using RO under anaerobic conditions [9]. Under the OSRO concept pre-treatment is minimal (only cartridge filters are used). However, using RO as an alternative to conventional water treatment methods is still limited due to the reasons mentioned above. In addition, water produced via RO can be corrosive to the water distribution piping network since it is slightly acidic (pH 5.5–6.0), has a low buffering capacity and is undersaturated with a negative LSI (Langelier Saturation Index) value. Furthermore, RO permeate is low in minerals content and although, neither WHO nor the European Water Directive set a limit for hardness in water, several EU countries have imposed via regulations or technical guidelines a limit on water hardness. For example, a minimum of 1.0 mM water hardness is needed according to the water quality regulations in the Netherlands (where this study is investigated) [10]. Therefore, to protect the integrity of the water distribution network and to meet the water quality standards, RO permeate post-treatment i.e., remineralization is necessary. Remineralization means adjusting the water hardness by adding Ca^{2+} and/or Mg^{2+} and alkalinity to ensure better buffering capacity and increased mineral content. Remineralized reverse osmosis permeate is less aggressive toward the piping network [11].

Conventional reverse osmosis permeate remineralization processes include: chemical dosing, typically dosing $Ca(OH)_2$ followed by CO_2 [12,13], blending i.e. mixing RO permeate with partially (un)treated feed water [14], and dissolving $CaCO_3$ using calcite filters to increase the Ca^{2+} content, followed by pH adjustment using NaOH [15,16]. The downsides of using these methods involve the additional use of chemicals, which brings an extra cost and has a higher environmental impact (less sustainable), suboptimal control on the final water quality due to mixing with partially or untreated feed water, and higher mechanical work due to frequent replacement of the calcite material, respectively. Most of the RO conventional remineralization methods are focused on external chemicals or product addition, whereas feed water originally already contains the remineralization components (calcium and magnesium). Therefore, several researchers proposed more cost-effective solutions for RO permeate remineralization by isolating divalent ions from the source water [17–20].

Nativ et al. [17] used nanofiltration (NF)–Dia-nanofiltration (DiaNF)–electrodialysis (ED) hybrid process for the selective removal of magnesium from seawater. NF was used to provide an Mg^{2+} rich retentate, which subsequently was treated with DiaNF for monovalent ions removal. The resulting stream finally was concentrated via ED resulting in a low Cl^-:Mg^{2+} ratio of 0.2. However, the Cl^-:Mg^{2+} ratio was found to be dependent on the ED filtration time and the ion exchange membranes selectivity. Birnhack et al. [18] used a quite similar approach for concentrating Mg^{2+} and lowering the amount of monovalent ions in the remineralization stream, by applying a 3-step membrane filtration process using tight UF–NF–DiaNF. The authors did not specify the amount of antiscalant that would end up in the remineralised water. Philibert et al. [19] applied assisted reverse electrodialysis (A-RED) for salts recovery from surface water RO brine to remineralize the corresponding permeate. The resulting A-RED permeate stream was used to increase RO permeate hardness. Although nonconventional RO remineralization methods were shown to be competitive to currently applied methods, their application is limited to a small (lab) scale. The large-scale application of nonconventional RO remineralization methods is still limited due to several uncertainties, among which, are final water quality (remineralizing stream purity), antiscalant leakage, and energy requirements [21].

A new remineralization process based on reverse osmosis as the main treatment step was developed using a combination of ion exchange and bipolar membrane electrodialysis (BMED) processes [22]. The developed process is advantageous to the conventional RO remineralization processes discussed earlier, in terms of on-site application, reduced external chemicals use and better control of the final water quality. The source water of the developed process scheme shown in Fig. 1 is supposed to be (fresh) groundwater from Oasen drinking water treatment plant in Kamerik, the Netherlands. The groundwater mainly contains calcium, magnesium, ammonium and potassium (the groundwater composition can be found in Table S1 in the supplementary data. Iron and manganese were excluded from this study due to practical reasons for testing under anaerobic conditions.

Amberlite IRC748 weakly acidic chelating cation exchange resin (CEX) was (initially in sodium form) used as RO pre-treatment to selectively remove calcium and magnesium from feed water. Amberlite removal of bivalent non-carbonate hardness ions like Ca^{2+} and Mg^{2+} would lower the RO scaling potential and hence could increase RO recovery to >95 % in theory. By applying a gradient elution using HCl, the adsorbed calcium and magnesium ions can be selectively separated from other monovalent ions during the resin elution step. The resulting CEX elution stream partially is used for RO permeate remineralization. However, before using recovered salts ($CaCl_2$ and $MgCl_2$) in the remineralization process, the chloride anion must be exchanged into bicarbonate to avoid exceeding the chloride limit (150 mg/L, according to the WHO [23]) downstream and to increase the pH and buffering capacity of produced permeate. This is done by using an anion exchange resin (AEX), initially in the bicarbonate form. The cation and anion exchange processes will be batch-operated consecutive sequences. At the same time, using RO retentate as feed water for the bipolar membrane electrodialysis (BMED), HCl and NaOH needed for the elution/regeneration of both cation and anion exchange resins, respectively, will be produced. An external source of carbon dioxide is needed to generate the $NaHCO_3$ solution required for the AEX resin regeneration. Part of the NaOH produced will be needed to regenerate Amberlite IRC78 to Na^+ form after the elution step with HCl. It is necessary to operate the CEX in the Na^+ form in order not to lose the Amberlite IRC78 (weakly acidic resin) capacity under acidic conditions induced by H_3O^+ release if the CEX is operated in H^+ form. Amberlite IRC748 was selected based on earlier work, where the equilibria and kinetics of selected ion exchange resins were investigated to choose a resin that matches the remineralization process requirement [24]. The separation of divalent/monovalent (calcium and potassium as a case study) using AMBERLITE IRC748 resin and the purity/yield of the recovered fraction was thoroughly investigated in an earlier publication by testing various elution profiles [25].

This study sets out to investigate the feasibility of combining ion exchange resin and bipolar membrane electrodialysis processes for the recovery of Ca^{2+} and Mg^{2+} for reverse osmosis permeate remineralization. The study presents an individual investigation of each of the three processes (CEX, AEX and BMED) that form the developed remineralization scheme. Where, the effect of several operational parameters such as CEX loading and elution hydrodynamics, pH effect on AEX loading and potential calcium carbonate scale formation, and HCl and NaOH production at high concentrations using BMED are studied. Moreover, the interplay and trade-off between the different components forming the remineralization scheme given predefined criteria, operation limits, and performance are evaluated.

2. Materials and methods

2.1. Analysis apparatus and chemicals

A Metrohm ECO IC ion chromatography device provided with a C6 cation, Asupp 17 anion and Metrosep organic acids columns were used for anions (Cl^-, SO_4^{2-} and HCO_3^-) and cations (K^+, Na^+ and Ca^{2+}) concentration analysis in the gathered samples. The eluents used in the analysis processes – according to manufacturer recommendations – were 4 mM HNO_3, (5 mM Na_2CO_3 + 0.2 mM $NaHCO_3$) and 0.5 mM H_2SO_4, for cation, anion, and organic acid columns, respectively. For solution titration, A Metrohm 805 Dosimat device was used. Analytical grade NaCl, $NaHCO_3$, $CaCl_2{\cdot}2H_2O$, HCl (37 %), and NaOH chemicals were obtained from Sigma-Aldrich (Darmstadt, Germany). Solution preparation and dilution were done using ultra-pure Milli-Q water (Millipore).

2.2. Ion exchange

The equilibrium and kinetics of chosen cation and anion exchange resins were studied in batch and column experiments. The Amberlite IRC748 weakly acidic chelating cation exchange resin was selected since it has superior selectivity to divalent ions and exceptionally low selectivity for monovalent ions such as ammonium and potassium. Moreover, Amberlite IRC748 showed the fastest sorption kinetics among the tested resins [24]. More details about the cation resin selection criteria and physical and chemical characteristics are mentioned in previous work [24]. Two anion exchange resins DOWEX MARATHON A Type 1 and DOWEX MARATHON A2 Type 2 were chosen to investigate chloride-bicarbonate sorption equilibria and selectivities. The physical and chemical properties of the anion exchange resins can be found in the supplementary data (Table S2).

2.2.1. Ion exchange equilibrium

Equilibrium experiments were done to determine DOWEX MARATHON A Type 1 and DOWEX MARATHON A2 Type 2 anion exchange resins (initially in chloride form) selectivity toward bicarbonate. The anion exchange resins (AEX) were first conditioned to remove any manufacturing impurities and change the AEX resins into bicarbonate form. The AEX resin was regenerated with an excess of 1 M NaCl solution in an ion exchange column and then converted to the bicarbonate form using an excess of 1 M $NaHCO_3$. Finally, it was washed with demineralized water and stored for later use.

The sorption isotherms for both DOWEX MARATHON A Type 1 and DOWEX MARATHON A2 Type 2 were measured by contacting a varied dose of anion exchange resins (HCO_3^- form) with a fixed solution volume (100 mL) of 10 mM $CaCl_2$ solution. Sorption equilibrium experiments were done in triplicate at room temperature (~22 °C). The resin dose can be calculated as follows:

$$Resin\ dose\ (\%) = \frac{m_d \times q_m}{V \times C_0 \times z_i} \times 100 \tag{2.1}$$

where m_d is the resin dry mass (g), q_m is the resin dry capacity (meqv/g), V is the solution volume (L), C_0 is the initial solution concentration (mM) and z_i is the ionic valence.

DOWEX MARATHON A was used later in this research since it has a

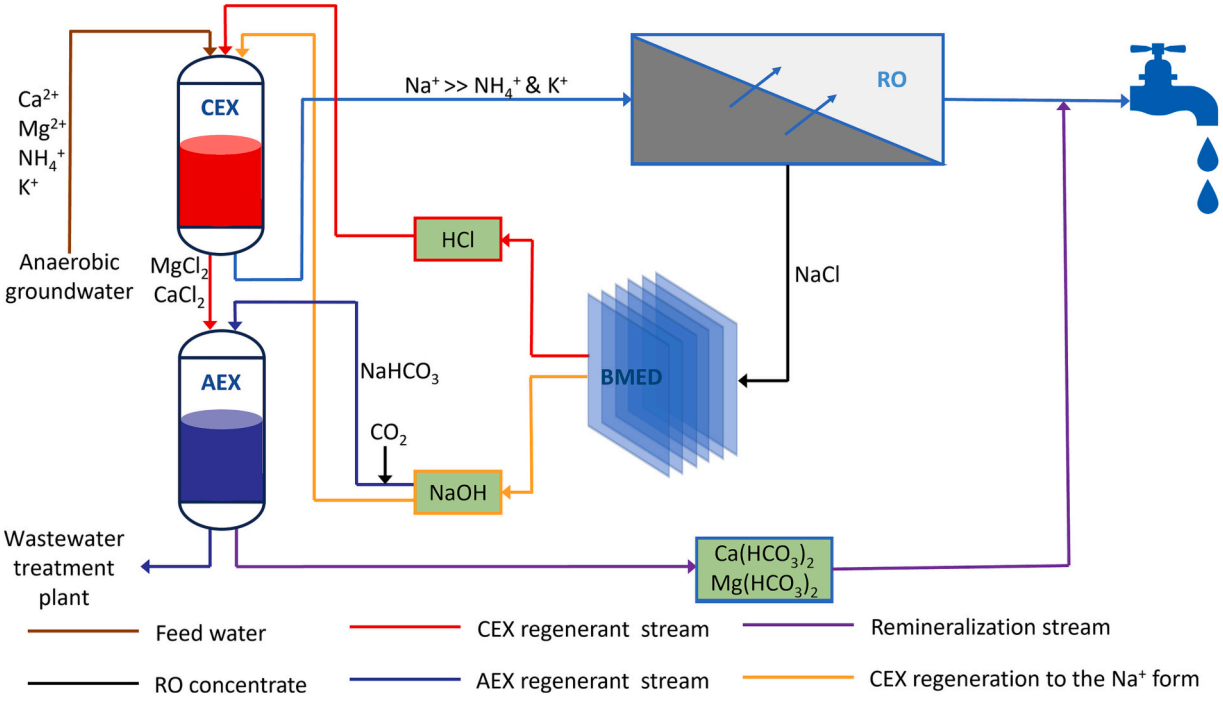

Fig. 1. The developed reverse osmosis permeate remineralization scheme combining ion exchange and bipolar membrane electrodialysis processes. The cation exchange regenerant including recovered magnesium and calcium is partially used for RO permeate remineralization. The anion exchange resin is used to convert chloride into bicarbonate. At the same time, HCl and NaOH are required to regenerate the ion exchange resins produced using BMED in the RO concentrate that has high NaCl content. Both ion exchange processes will be batch operated in consecutive steps [22].
The scheme is adapted from [24,25] with permission.

higher exchange and regeneration performance in waters with high CO_2 content which is the case in the remineralization process as will be explained later. More details about the selection criteria and both anion exchange resins sorption isotherms can be found in the supplementary data (Fig. S1).

A series of batch equilibrium experiments were done to study the effect of feed solution pH on the potential formation of calcium carbonate precipitates during the loading of calcium chloride on DOWEX MARATHON A anion exchange resin initially in HCO_3^- form. A series of 250 mL glass bottles were filled with 1.11 g of DOWEX MARATHON A AEX resin and 100 mL solution of 10 mM $CaCl_2$ concentration at varied initial solution pH. The resin dose used in the equilibrium experiments matched a max. of 75 % removal to make it possible to measure the remaining calcium or chloride at equilibrium. The pH of the different solutions was 0, 4, 6, 8, and 10. The solution pH was initially adjusted using 0.1 M NaOH solution. During the experiment, the solution pH was not corrected. The glass bottles were then placed on a magnetic stirrer at 180 rpm and ran for 24 h. After that, samples were taken from each glass bottle and filtered using a syringe filter provided by a 0.45 μm Whatman nylon membrane to avoid clogging the ion chromatography column. The filtered samples were analyzed for Ca^{2+}, Cl^- and HCO_3^- content using an ion chromatography device. Finally, the percentage of calcium precipitated was calculated as follows:

$$Ca^{2+}\ \text{precipitation}\ (\%) = \frac{C_0 \times V_0 - C_e \times V_e}{C_0 \times V_0} \times 100. \tag{2.2}$$

where C_0 is the initial solution concentration (mM), V_0 solution initial volume (L), C_e solution concentration at equilibrium (mM), and V_e solution volume at equilibrium (L).

2.2.2. Column experiments

Cation and anion exchange resins were tested in a lab-scale ion exchange set-up. A detailed description of the ion exchange set-up, typical ion exchange cycle (loading and elution) and columns used can be found in previous work [25]. Column experiments were done in triplicate and at room temperature (~22 °C).

2.2.2.1. Cation exchange. A lab-scale ion exchange column K26/40 (Diameter (d) = 26 mm, Column height (H) = 40 cm) (adjusted to operate at a higher flow rate (>10 m/h) (Cytiva Life Sciences, the Netherlands) was filled with 105 g wet Amberlite IRC78 (Na^+ form, bed capacity = 1.42 equivalent (eq)/L). 1 M HCl and 1 M NaOH were used to pretreat the resin material to remove manufacturing process impurities remains, such as sodium leftovers from the resin regeneration during the manufacturing process. The column was operated in a co-current mode for practical reasons; operating in co/counter current was shown not to affect the regeneration efficiency [25]. The ion exchange cycle included the following steps, accordingly: loading with $CaCl_2$ at 5 m/h (empty bed contact time (EBCT) = 3.23 min), elution with HCl at 1 m/h, 3 bed volumes (BV) regeneration with 1 M NaOH at 1 m/h, 1 BV slow rinse at 1 m/h, 5 BV fast rinse at 5 m/h, 2 BV backwash at 1.6 m/h. the slow, fast rinse and backwash were done with demineralized water. The slow and fast rinse was applied after the elution and regeneration cycles, while the resin backwash was applied before loading the resin material. The slow rinse was applied to allow for further resin regeneration and conversion. The fast rinse was applied to clean the resin bed from the eluent solution and prepare for the next ion exchange cycle. Samples were collected at the ion exchange column outlet and analyzed using the aforementioned ion chromatography device. Then, ion exchange breakthrough curves were used in assessing the influence of hydrodynamics on the ion exchange process performance. Furthermore, varied elution profiles were used to investigate the separation of divalent and monovalent ions (calcium and potassium as a case study) during the resin elution step. The purity and yield curves resulting from each elution profile tested were then compared. A detailed description of the elution profiles tested and the purity and yield calculations can be found in earlier work [25].

2.2.2.1.1. Thomas model. Frontal analysis using the Thomas model, which assumes a limited number of equilibrium stages (but no mixing between stages) and a mass transfer rate directly proportional to the deviation from phase equilibrium (constant selectivity coefficient), was used to correlate the breakthrough data and to determine the kinetic constant (k_{ad} (L/eqv·s)) and column plate number (N_r) [26]. The Thomas model form given by Vermeulen and Hiester [27] was used to fit the ion exchange breakthrough curve,

$$\frac{C}{C_0}(T, N_r) = \frac{J(N_r r^*, N_r T)}{J(N_r r^*, N_r T) + [1 - J(N_r, N_r T r^*)]\, e^{[(1-r^*)(N_r - N_r T)]}} \tag{2.3}$$

where the J-function is defined with the modified Bessel function I_0 by

$$J(x, y) = 1 - e^{-y} \int_0^x e^{(-\xi)} I_0\left(2\sqrt{y\xi}\right) d\xi \tag{2.4}$$

N_r is the column plate number related to reaction adsorption rate kinetics and calculated as follows,

$$N_r = k_{ad} Q_{max} \frac{L}{u_s} \tag{2.5}$$

where L is the column length (m), k_{ad} is the kinetic constant (L/eqv·s), Q_{max} is the maximum resin capacity in (eqv/L), and u_s is the superficial velocity (m/s).

r^* is phase equilibrium parameter calculated as follows,

$$r^* = \left(1 + \frac{C_0}{K_d}\right)^{-1} \tag{2.6}$$

T is a dimensionless time calculated as follows,

$$T = \frac{C_0}{Q_0} \frac{u_s}{L} \left(t - \frac{L\varepsilon_b}{u_s}\right) \tag{2.7}$$

where C_0 and Q_0 are the initial concentration (M) and corresponding equilibrium capacity (eqv/L) ($Q_0 = \frac{Q_{max} \times C_0}{K_d + C_0}$), K_d, is the equilibrium constant for the isotherm ($= k_{des}/k_{ad}$), mg/mL), respectively, t is the time in (s) and ε_b is the bed packing porosity.

2.2.2.2. Anion exchange. The same ion exchange setup described earlier was loaded with 55 g of DOWEX MARATHON A type 1 wet anion exchange resin (Cl^-, bed capacity = 1.3 eq/L). Similarly, the anion exchange resin was first pre-treated to remove manufacturing impurities with 1 M NaCl and later excess of 1 M $NaHCO_3$ to convert it to the bicarbonate form. The anion exchange cycle included the following steps: loading with 10 mM $CaCl_2$ at 5 m/h, 3 BV regeneration with 1 M $NaHCO_3$ at 1 m/h, 1BV slow rinse at 1 m/h, 5 BV fast rinse at 5 m/h and 2 BV backwash at 1.60 m/h. Occasionally, an extra rinsing step with 1 M HCl acid solution at 5 m/h for 2 BV was used after the loading step to remove any calcium precipitates that might be formed. Samples were collected at the column outlet and the pH was recorded in time. Collected samples were filtered using a syringe filter provided by a 0.45 μm Whatman nylon membrane before being analyzed with the ion chromatography device to avoid clogging the ion chromatography column with potential calcium precipitates.

2.2.3. Bipolar membrane electrodialysis

A lab-scale bipolar membrane electrodialysis (BMED) stack FT-ED-100 (FUMATECH BWT GmbH, Germany) of a nominal membrane area 10 × 10 cm (100 cm^2) and equipped with 2 cell pairs (repeat units) was used in studying the bipolar membrane process performance. A unit cell pair is formed from a Fumasep FKB-PK-130 cation exchange membrane, a Fumasep FAB-PK-130 anion exchange membrane and a Fumasep FBM bipolar membrane provided by FUMATECH BWT GmbH, Germany. FAB and FKB membranes are specifically designed for BMED applications and have pH stability of 0–14. In addition, FAB and FKB membranes are

characterized by high H_3O^+ and OH^- retentions, respectively. The BMED was operated in batch mode where 0.5 M Na_2SO_4 electrode rinse solution, NaCl feed solution, HCl, and NaOH solutions were circulating until it was impossible to keep a constant current applied. The BMED experiments were done at 15 °C using a cooling bath to mimic the groundwater average temperature. The bipolar membrane was used in reverse bias configuration, i.e., the bipolar membrane cation exchange side was facing the cathode to ensure H_3O^+ and OH^- flow outside the bipolar membrane layers and avoid water blisters in the anion or cation membrane layer and hence damaging the membrane surface area [28]. The initial concentration of HCl and NaOH used in the BMED experiment was 0.1 M. Current supply was provided using potentiostat SM 120 – 25 D (Delta Elektronika B.V., the Netherlands), which has an electric current and potential range of 0–25 A and, 0–120 V, respectively. The salt cation (Na^+) passes through the cation exchange membrane to the base compartment where it combines with hydroxyl ions produced by BPM to form NaOH. Similarly, the salt anion (Cl^-) passes through the anion exchange membrane to the acid compartment where it combines with hydrogen ions produced by BPM to form HCl. Therefore, the process yields HCl acid and NaOH in equimolar amounts using NaCl as a feed solution presuming that the current efficiency (the amount of current which is converted into valuable products) is 100 %. If the current efficiency is lower than 100 %, counter ions might leak to the wrong compartment and product purity lowers. A more detailed description of the BMED setup can be found in earlier work [29].

3. Results and discussion

3.1. Cation exchange process

The effectiveness of the ion exchange process is governed by the exchange equilibria, kinetics, and hydrodynamics. Both cation exchange equilibria and kinetics were described in detail before [24]. The following sections investigate the effect of the cation exchange process hydrodynamics in terms of loading flow rate and solution concentration on the obtained breakthrough curve. Furthermore, the monovalent/divalent separation process in terms of recovered fraction purity and yield is studied using multiple elution profiles.

3.1.1. Effect of loading flow rate on cation exchange column efficiency

In a fixed-bed column experiment, the effect of feed solution loading flow rate on the cation exchange process was investigated. Amberlite IRC748 (Na^+ form) weakly acidic chelating cation exchange resin was loaded with 25 mM $CaCl_2$ solution at different superficial loading velocities of 1.0, 5.0 and 10.0 m/h. The cation exchange performance was evaluated using the breakthrough curve obtained at the column outlet. The breakthrough curve (Fig. 2) shows the change in fractional calcium concentration as a function of dimensionless time (T) defined earlier.

The plate theory discussed by several researchers [30–32] was used to describe the column efficiency at multiple loading flow rates. According to the plate theory, the ion exchange column is divided into stages where the equilibrium between ions in the solution and ions attached to the resin functional group exists [30]. The plate height is related to the column number of plates (N_r) as follows,

$$HETP = \frac{L}{N_r} \tag{3.1}$$

where *HETP* is the plate height (m).

The higher the plate number the lower the broadening of the wavefront during its propagation in the column and the more efficient the utilization of the bed capacity [33]. Wavefront broadening occurs due to different transport rate resistances such as ion exchange rate, film diffusion and intraparticle diffusion [30]. The applied Thomas model considered only the effect of the ion exchange rate on the column number of plates.

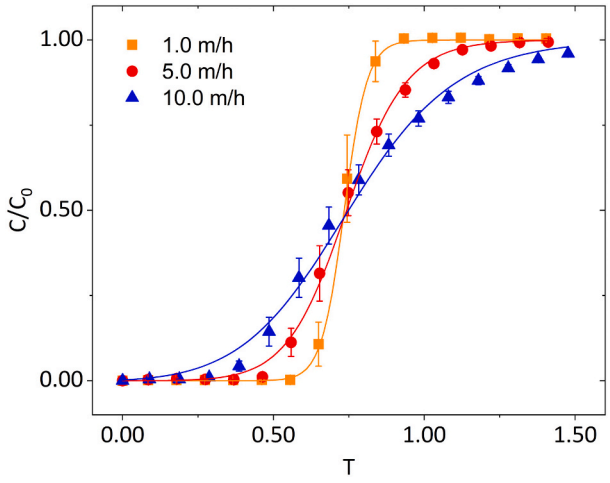

Fig. 2. Calcium breakthrough curves at different superficial loading velocity. The lines are Thomas model fitting. C_0 = 25 mM $CaCl_2$, room temperature (~22 °C), H = 0.4 m. T is the dimensionless time.

Fig. 2 shows that sharper breakthrough curves were obtained experimentally at lower flow rates. As expected, a higher plate number was calculated at lower velocities (Table 1); yet ion exchange kinetics were higher at a higher loading rate. Van Deemter et al. [30] showed that wave broadening due to resistance to mass transfer i.e., ion partitioning between the liquid and solid phase, is more evident at a higher velocity and can be minimized substantially by lowering the wavefront velocity. Broadening due to a limited mass transfer rate is partially counteracted by a phenomenon called "self-sharpening", which originates from the non-linearity of the ion exchange equilibrium function. The self-sharping wavefront means that the lagging wavefront at a higher solution concentration (wavefront upstream) moves faster than the leading wavefront at a lower solution concentration (wavefront downstream). A self-sharpening ion-exchange breakthrough curve is essential for a better ion exchange performance. A sharper breakthrough curve means higher utilization of the ion exchange capacity and postponing the ions breakthrough and fewer regeneration cycles are needed.

3.1.2. Effect of loading solution concentration on cation exchange column efficiency

The effect of the feed solution concentration on the cation exchange process was investigated in a fixed-bed column process. The Amberlite IRC748 weakly acidic cation exchange resin was loaded with $CaCl_2$ solution at different concentrations and a constant loading flow rate of 5.0 m/h. The breakthrough curve obtained at different loading solution concentrations is shown in Fig. 3. The breakthrough experimental data were fitted using the frontal analysis Thomas model discussed earlier. The calculated kinetic constant and the related column plate number are shown in Table 2.

Fig. 3 clearly shows that the sharpness of the breakthrough curve was significantly improved by decreasing the feed solution concentration, i.e., higher utilization of the column capacity was achieved at a lower feed

Table 1
Calculated kinetic constant k_{ad} and the 95 % confidence intervals using the Thomas model for fitting the experimental cation exchange breakthrough data at different loading velocities. The column plate number for adsorption kinetics (N_r) rounded to the nearest integer, was calculated using Eq. 2.5.

Loading velocity (m/h)	Kinetic constant k_{ad} (L/eqv·s)	Column plate number (N_r)
1.0	0.0226 ± 0.0044	30.0
5.0	0.0416 ± 0.0041	11.0
10.0	0.0451 ± 0.0043	6.0

solution concentration. Moreover, Table 2 shows that the column plate number and the kinetic coefficient increased with decreasing feed solution concentration. This can be attributed to the fact that resin selectivity is much higher in dilute solutions (low concentration) compared to high solution concentrations. This is true in the case that the solution counter ion and the ion attached to the resin functional group have an unequal charge (calcium is divalent and sodium is monovalent). Total solution concentration affects the ion exchange equilibrium significantly. This can be seen in the sorption isotherm according to the mass action law (Eq. 3.2). For monovalent-divalent ion exchange (calcium and sodium in this case), lowering the total solution concentration indicates a higher initial sorption isotherm slope (more counter ions in the resin material) and hence faster sorption [25]. This means lower propagation velocity of the concentration front and hence increasing the column plate number and improving the breakthrough curve self-sharpening. A similar result was obtained by Myers and Byington [34] in the case of copper and sodium using cation exchange resin Dowex 50-X8 at different bulk solution normality.

$$K_{A,B} = \left(\frac{C}{Q}\right)^{n-1} \frac{y_A(1-x_A)^n}{y_A(1-x_A)^n} \tag{3.2}$$

where $K_{A,B}$ is the molar selectivity coefficient, C is the total solution concentration, Q is the total resin capacity, n is the charge ratio of ions A and B, x_A and y_A are the equivalent ion fractions in solution and resin respectively.

In accordance with Figs. 2 and 3, improving the cation exchange process efficiency and hence the total remineralization process performance can be achieved by loading the cation exchange resin with a dilute solution concentration and at a lower loading rate. Total calcium and magnesium concentration in the (fresh) groundwater used is around 3 mM, therefore, a sharp and self-sharpening breakthrough curve is expected. However, at the industrial large scale, cation exchange resins are usually operated at loading flow rates in the range of 5–60 m/h, which could affect this sharpness. Therefore, as has been mentioned earlier and according to Van Deemter et al. [30], the wave broadening due to resistance to mass transfer is more evident at a higher velocity, which results in less loading efficiency, i.e., sooner breakthrough of the ion exchange curve, less efficient use of the resin capacity and frequent regeneration, which implies more chemical use. Therefore, a pilot scale evaluation or process simulation should be performed to assess the breakthrough curve at such high loading rates and the process economic feasibility.

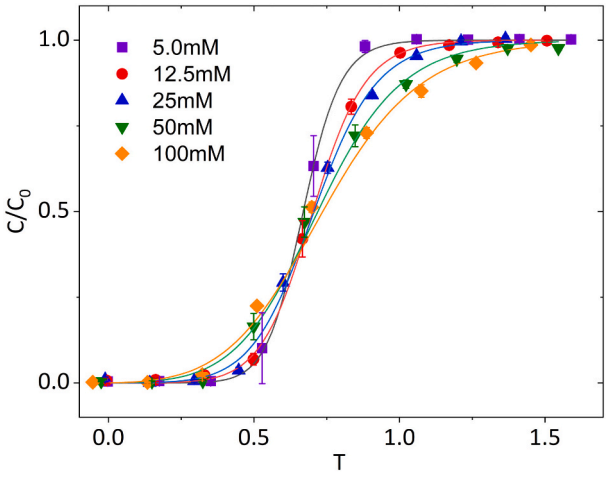

Fig. 3. Calcium breakthrough curves as a function of time at different loading solution concentrations. The connected lines are Thomas model fitting. $u_s = 5$ m/h, room temperature (~22 °C), H = 0.4 m. T is the dimensionless time.

Table 2
Calculated kinetic constant k_{ad} and the 95 % confidence intervals using the Thomas model for fitting experimental cation exchange breakthrough data at different feed solution concentrations. The column plate number (N_r) rounded to the nearest integer, was calculated using Eq. 2.5.

Loading concentration (mM)	Kinetic constant k_{ad} (L/eqv.s)	Column plate number (N_r)
5.0	0.075 ± 0.02	20.0
12.5	0.049 ± 0.005	13.0
25.0	0.041 ± 0.003	11.0
50.0	0.030 ± 0.003	8.0
100.0	0.026 ± 0.002	7.0

3.1.3. Isocratic and gradient elution of cation exchange column

The Amberlite IRC748 chelating weakly acidic cation exchange resin is now mainly loaded with hardness ions and traces of monovalent ones. Since the cation exchange process is stoichiometric and reversible, the recovery of sorbed calcium and magnesium during resin elution is possible. The eluent used in the elution process is hydrochloric acid since protons are capable of breaking chelating bonding between counterions and resin functional groups in weakly acidic chelating resins [35]. Commonly, an isocratic elution profile – i.e., a constant total eluent ionic strength – is used for ion exchange resin regeneration. However, for chromatography (ion separation/fractioning) purposes, gradient elution has shown better potential in acquiring higher purity and yield fractions [36,37]. During gradient elution, the eluent concentration is continuously changing in time which affects the ions desorption rate and equilibrium with the resin material dramatically. In gradient elution, the sorption isotherm shape is considered constant and independent of concentration, yet the molar selectivity coefficient is concentration-dependent [33]. A detailed investigation of the Amberlite IRC748 elution process in terms of elution flow rate, concentration and operation mode can be found in [25].

The separation of calcium from potassium (as a case study) in a partially loaded Amberlite IRC748 resin (Na^+ form) using different elution profiles was studied. The ion exchange column was loaded with a solution containing K^+ and Ca^{2+} in a 60:40 mole ratio, which simulates the worst-case separation scenario where monovalent ions are higher in concentration compared to divalent ions. The different elution profiles experiments were done at room temperature using a similar total eluent moles solution concentration. The purity and yield of the recovered calcium fraction are shown in Pareto frontiers Fig. 4 using gradient (linear and stepwise) and non-gradient isocratic elution profiles. Fig. 4 shows that better separation of the recovered calcium (i.e., higher yield at the same purity) was achieved using gradient elution profiles than non-gradient elution profiles. The purity and yield of the calcium recovered were higher using the linear gradient elution profile compared to the stepwise elution profile. This is expected since the linear elution profile is formed of infinite concentration steps.

Eluted component wave propagation velocity across the column length is dependent on both the resin selectivity (sorption isotherm slope) and the eluent concentration. In an earlier work [24] it was shown that Amberlite IRC 748 has superior selectivity for divalent ions (calcium) than monovalent ones (potassium). The resulting molar selectivity coefficient ($K_{ion/Na+}$) from mass action law fitting of calcium and potassium sorption isotherm was 2574 ± 1100, and 0.53 ± 0.3, respectively [24]. This implies that a slower propagation velocity is expected for calcium than for potassium at the same eluent concentration. Hence, a lagging period occurs between desorbed potassium and calcium wavefronts, and as a result, less peak overlap occurs, and the separation is substantially improved. As the eluent concentration gradually increases, the desorption of the more selective ion (calcium) will be accelerated until complete elution. Therefore, gradient elution might be a promising elution method that can be used in tuning the eluted components desorption rate and achieving improved separation. Furthermore, by applying the same quantity of eluent, gradient elution

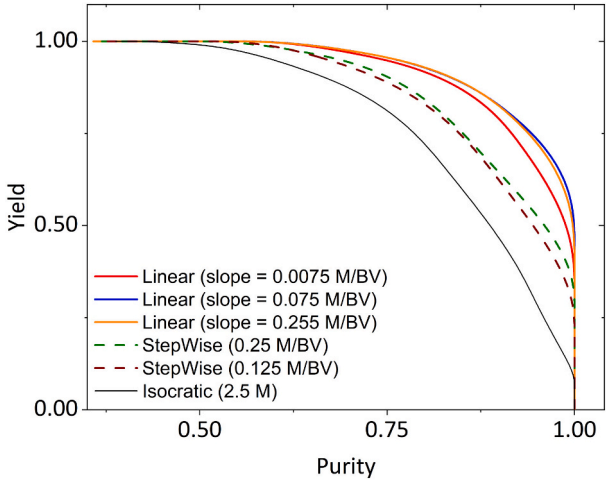

Fig. 4. Pareto frontiers of the purity and yield of the separated calcium fraction using a gradient (linear and stepwise) and non-gradient conventional isocratic elution profiles.
Adapted from [25] with permission.

was shown to be superior to conventional isocratic elution in achieving better monovalent-divalent ion separation in higher purity and yield.

3.2. Anion exchange process

The anion exchange process in the developed RO permeate remineralization scheme plays a complementary role to the cation exchange process. Anion exchange resin is applied to change calcium chloride into calcium bicarbonate. Since calcium carbonate/bicarbonate is sparingly soluble in water ($CaCO_3$ solubility = 6.6 mg/L at 20 °C [38]) adjusting and understanding the effect of loading solution pH on the carbonate equilibrium is necessary to prevent potential carbonate scaling on the resin material. The effect of feed solution pH on the carbonate equilibrium during the anion exchange cycle was studied both in batch and column experiments and will be discussed in the following sections.

3.2.1. Effect of initial feed solution pH on anion exchange process efficiency (batch experiment)

Potential calcium carbonate deposit formation on the anion exchange resin DOWEX MARATHON A (HCO_3^+ form), when contacted with calcium chloride solution, was investigated in a batch experiment. A fixed concentration of 10.0 mM $CaCl_2$ was equilibrated with 1.11 g of DOWEX MARATHON A AEX resin to obtain 75 % maximum removal at varied initial solution pH. The solution pH was not adjusted during the equilibration process. Fig. 5 shows the percentage of the calcium precipitated as a function of the initial solution pH, in addition, to the final solution pH at equilibrium. The graph shows that, for equilibrium experiments with an initial solution of pH ≥ 4, around 50 % of the calcium in the original solution was precipitated. In contrast, no calcium precipitation was observed when the initial solution pH was lowered to zero. Moreover, the final solution pH at equilibrium was the same for all the experiments (pH = 7.0) except for the case where the initial solution pH was equal to 0, where the equilibrium pH was similar to that in the initial state (pH = 0).

Bicarbonate released from the anion exchange resin during equilibrium with chloride can either stay in the bicarbonate form or shift to carbonic acid H_2CO_3 (below $pK_1 = 6.37$) or carbonate CO_3^{2-} above $pK_2 = 10.36$ depending on the local solution pH according to the Bjerrum plot [39,40] (supplementary data Fig. S2). $pK_1 = pH = 6.37$ is the point of equal concentration of H_2CO_3 and HCO_3^- and $pK_1 = pH = 10.36$ in the equivalence point of concentration of HCO_3^- and CO_3^{2-}. For the experiments with an initial solution pH between 4 and 10, the equilibrium solution pH was around 7. According to the Bjerrum plot, mostly

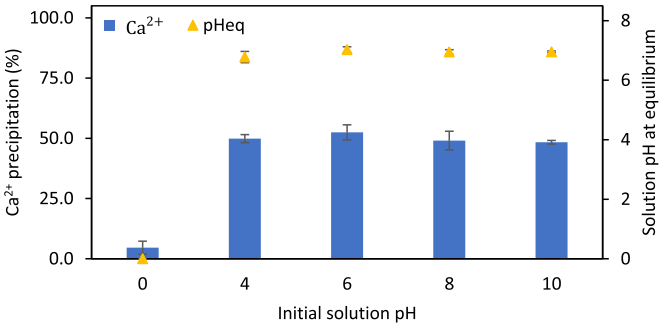

Fig. 5. The effect of initial solution pH on the formation of calcium carbonate deposits during the exchange of chloride for bicarbonate in anion exchange resin DOWEX MARATHON A. Temperature = 22 °C, [Cl^-] = 10 mM, wet resin weight = 1.11 g.

bicarbonate should exist, and no carbonate deposits should form. Yet, almost half of the calcium present at the beginning of the experiment was precipitated. This can be due to an increase in the local pH around the resin bead to a $pK_2 \geq 10.36$ where carbonate is the most prevalent form. However, the local pH around the resin bead was marginally affected during the release of bicarbonate in exchange for chloride ions when lowering the bulk solution pH to 0. Therefore, only bicarbonate/carbonic acid was formed, and hence very little calcium carbonate precipitation was observed. Calcium carbonate formation at the resin material can block the exchange sites and hence lower resin capacity and increase the pressure drop across the column. Therefore, Fig. 5 shows that feed solution pH adjustment is necessary during chloride/bicarbonate exchange using the anion exchange process.

3.2.2. Effect of feed solution pH on anion exchange process efficiency (column experiment)

The effect of feed solution pH on potential calcium carbonate scale formation as a result of chloride/bicarbonate exchange using DOWEX MARATHON A anion exchange resin was investigated in a column experiment. Fig. 6 shows the yield of the collected calcium and bicarbonate at the column outlet during the loading step. Calcium and bicarbonate yields were calculated from the breakthrough curves obtained as follows:

The resin capacity at exhaustion i.e., complete chloride breakthrough (q) was calculated using Eq. 3.3

$$\text{Resin capacity } (q) = \frac{C_{0,cl} \times Q}{\frac{m}{\rho_r}} \times \int_{t=0}^{t_{c=c_{0,cl}}} \left(1 - \frac{C}{C_{0,cl}}\right) dt \qquad (3.3)$$

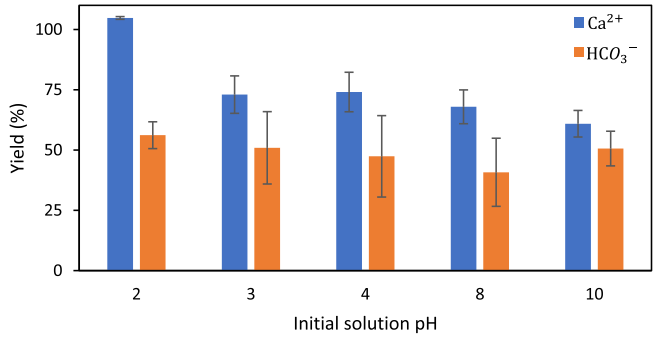

Fig. 6. The effect of initial solution pH on the calcium and bicarbonate yield during calcium chloride loading on DOWEX MARATHON A anion exchange resin initially in bicarbonate form. Temperature = 22 °C, [$CaCl_2$] = 10 mM, wet resin weight = 53.80 g.

$$\text{Calcium yield } (Y_{Ca}) = \frac{\int_{t=0}^{t_{c=c_{0,cl}}} \frac{C_{ca}}{C_{0,ca}}\, dt}{t_{c=c_{0,cl}}}, \tag{3.4}$$

$$\text{Bicarbonate yield } \left(Y_{HCO_3}\right) = \frac{\int_{t=0}^{t_{c=c_{0,cl}}} C_{HCO3}\, dt}{\frac{m}{\rho_r} \times q} \tag{3.5}$$

where c is the breakthrough concentration of Cl^-, Ca^{2+} or HCO_3^- in mM, Q is the loading flow rate (L/h), c_0 is initial solution concentration in mM, t is breakthrough time (h), m is the resin wet weight (g) and ρ_r is resin apparent density in (g/L).

Fig. 6 shows that calcium yield was <100 % when the feed solution pH was higher than 2, yet, increased marginally as the solution pH decreased. Only at a solution pH of 2, all calcium was recovered during the anion exchange loading, and no calcium carbonate deposits were formed. Bicarbonate recovery, however, was around 50 % for all the pH ranges tested. These results indicate that the local pH around the resin bead was marginally affected during the release of bicarbonate in exchange for chloride ions even when lowering the bulk solution pH to 3. This resulted in calcium carbonate deposit formation and lowered both calcium and carbonate yields. However, at pH = 2, the local resin bead pH was apparently below the pK_1 and pK_2 in the Bjerrum plot shown in Fig. 6 and hence calcium carbonate deposits were not formed. The decrease in bicarbonate yield at pH = 2 can be attributed to carbonic acid formation at a very low solution pH. It can be concluded from Figs. 5 and 6 that a favorable feed solution pH < 3 exists where the formation of calcium deposits is prevented during chloride/bicarbonate anion exchange. The pH of the cation exchange regeneration stream that will be used for the remineralization of RO permeate (Fig. 1) would be around 0 since a high concentration of HCl is used in the CEX regeneration. Therefore, calcium deposit formation is not expected to occur, however, the bicarbonate yield and carbonic acid formation or CO_2 bubbles formation have to be monitored carefully and feed pH adjustment might be necessary.

3.3. Bipolar membrane electrodialysis: effect of feed solution concentration on acid and base production

Bipolar membrane electrodialysis (BMED) forms the third and last part of the remineralization process presented. BMED role in the developed remineralization scheme in the production of HCl and NaOH is needed for CEX and AEX resins regeneration from softened RO concentrate with a high concentration of NaCl. The process was investigated in detail by the authors in previous work for defined performance criteria such as product purity, yield, current efficiency and energy consumption at varied operational parameters including current density, flow rate and feed concentration [29]. It was concluded that BMED can be a viable solution to produce on-site HCl and NaOH at high purity and yield. However, the NaCl feed concentration tested was in the range between 0.1 and 1.0 M, which is far below commercially available HCl (37 % (w/w) = 12 M) and NaOH (50 % (w/w) = 18.94 M) solutions. Highly concentrated acid and base solutions are practically desirable since it uses less storage space and can be diluted later to acquire the desired concentration. Therefore, the viability of producing highly concentrated acid and base using BMED was investigated, and the results are given in Fig. 7.

Fig. 7 shows that HCl purity decreases significantly when the NaCl feed solution concentration increases to above 3.0 M. The HCl purity at a feed solution concentration <1.0 M is 97 % whereas at 3.0 M the HCl purity was 10 % lower (87 %). The decrease in HCl purity is mainly attributed to the high co-ion (Na^+) leakage into the acid compartment with a higher NaCl concentration used. Co-ion leakage is marginal up to 1.0 M where the NaCl concentration is less than the anion exchange membrane charge density (0.8–1.1 meqv/g) [41]. Higher feed solution concentration than membrane charge density implies lower membrane permselectivity due to less Donnan exclusion and hence increased co-ion

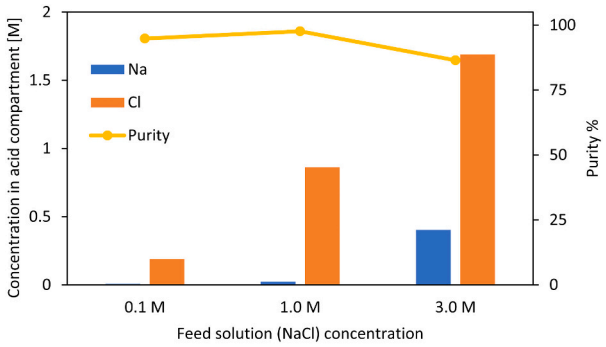

Fig. 7. Effect of feed solution (NaCl) concentration on the purity of HCl produced using BMED. Batch experiment done at current density = 1000 A/m^2, cross flow velocity = 7 cm/s.

leakage and lower product purity [42]. Similar behaviour was observed for the NaOH (Supplementary data Fig. S3), where higher NaCl concentration in the feed solution resulted in less pure NaOH at 3.0 M NaCl (95 %) compared to 1.0 M NaCl (85 %). This can also be attributed to the leakage of Cl^- co-ion through the cation exchange resin at higher feed solution concentration exceeding the cation exchange resin charge density (0.9–1.1 meqv/g) [41].

Not only that the product purity is lower at high feed solution concentration, but also the process current efficiency is lower due to the lower membrane permselectivity. The current efficiency for 0.1, 1.0 and 3.0 M NaCl feed solution was 94, 75, and 70 %, respectively. Energy consumption decreased from 11.70 to 9.90 kWh/kg acid produced when the feed solution increased from 0.1 to 1.0 M (the actual calculations of the current efficiency and energy consumption can be found in earlier work [29]). However, the energy needed at 3.0 M (9.82 kWh/kg) was similar to the 1.0 M case, which indicates that lowering the solution resistance (i.e., increasing feed solution concentration) further would marginally affect the total energy consumption. Hence energy use is mainly impeded in the current density applied.

Producing 1.0 M of HCl and NaOH with high purity (>95 %) using BMED would be sufficient to comply with the developed remineralization process requirements. Therefore, producing acid and base with higher concentration and hence lower purity will not be necessary. Part of the remineralization process is the regeneration of the anion exchange resin using $NaHCO_3$. The production of $NaHCO_3$ will be done by contacting NaOH with an external source of CO_2. The solubility limit of $NaHCO_3$ is around 1.0 M at 25 °C [38], and in order to not exceed this limit, the NaOH concentration should not be >1.0 M. Given the purity data shown in Fig. 7 and supplementary data (Fig. S3), the purity of 1.0 M HCl and NaOH produced is >95 %.

3.4. Remineralization process trade-off and cost

Understanding the interplay and recognizing the trade-off between the elements forming the presented remineralization process i.e., CEX, AEX and BMED is a crucial aspect in having a highly efficient process design with stable performance. This can be achieved by first understanding the remineralization process demands, operation limits and criteria.

3.4.1. Remineralization process trade-off and interplay

The presented remineralization process was developed for a "fresh" groundwater treatment process using reverse osmosis as shown in Fig. 1. As a result of applying the developed remineralization process, the recovery should be increased from 80 % (currently) to >95 % (in theory) due to the absence of the scale-forming divalent ions. Moreover, the RO permeate hardness should be adjusted to at least 1.0 mM water hardness following the Dutch standards. The RO feed water at Kamerik, the

Netherlands has 3.0 mM hardness, where in principle one-third of the hardness available would be used for RO product remineralization. In the presented remineralization process, the following main parameters are critical for the efficient operation of the different process components: NaCl concentration in source water, yield and purity of the recaptured components (magnesium and calcium) as well as HCl and NaOH (products of BMED process), pH of AEX feed water, and energy required. Furthermore, since the remineralization scheme is formed of multiple processes, a short highlight is described over predicting the large-scale operation.

The maximum HCl and NaOH concentration produced by BMED was limited to 1 M to avoid exceeding the solubility of the later-produced $NaHCO_3$ at 10.3 g/100 g at 25 °C. However, currently used fresh groundwater has a sodium concentration of ≈2.20 mM. If the RO is operating at >95 % recovery Na^+ concentration in the RO concentrate then would be in the range of 50–200 mM, therefore, the addition of extra NaCl to the RO concentrate water is required to obtain the 1 M NaCl concentration. Alternatively, a groundwater source with higher salinity (brackish) can be used as RO feed water to increase the NaCl concentration in the RO concentrate solution.

The final purity of the remineralization stream i.e., recovered hardness ions is governed by the purity of the BMED-produced HCl eluent and the effectiveness of the separation process during CEX elution. The purity of the 1.0 M HCl produced by BMED is affected by the leakage of sodium ions into the acidic compartment. Taking into account the WHO limits for sodium and chloride in drinking water of 200, and 250 mg/L, respectively [43], the purity of the 1.0 M HCl solution should be >99 %. The maximum purity obtained for 1.0 M HCl was around 98.8 % [29], similar to the purity required. Depending on the amount of hardness ions recovered, the purity of the remineralization stream can also be determined in line with WHO standards for sodium and chloride in the drinking water. In previous work, the calcium productivity achieved was around 200 mmol/L·h [25], with a purity of >95 %, which would result in sodium impurities higher than WHO limits. Yet, keeping in mind that only 1.0 mM hardness is needed for drinking water, a dilution factor should be applied, which would result in remineralized drinking water that complies with WHO standards for sodium and chloride. Therefore, it is still possible to use less pure HCl eluent or remineralize with a less pure remineralization stream than the limits defined above.

The pH of the CEX regenerant stream i.e., recovered hardness ions is crucial for the success of the AEX in exchanging chloride into bicarbonate. As has been discussed earlier, calcium precipitates might form as a result of bicarbonate release from the AEX resin in exchange for chloride. Since the eluting stream of the CEX contains 1.0 M HCl, the pH of the elution stream would be around 0. It has been shown before that operating the AEX under acidic conditions should eliminate the calcium carbonate precipitate formation potential. However, the formation of CO_2 bubbles and a lower bicarbonate yield is expected. Therefore, the AEX process should be optimized, in terms of feed pH or way of operation to facilitate the removal of CO_2 bubbles potentially forming.

BMED is the most energy-intensive element in the developed remineralization process. The energy required to produce 1.0 M HCl and NaOH is around 8.0 and 7.75 kWh/kg acid/base which is around 1.8 and 1.9 kWh/m^3 water produced (see supplementary data for more details), respectively. That is around twice as much as the energy needed for RO using fresh and brackish groundwater (0.5–1.0 kWh/m^3) [44]. However, chemical production on site and the low volume of the BMED-produced acid and base needed for ion exchange resin regeneration might still make BMED an attractive process for acid and base production. Nevertheless, BMED is still an energy-intensive product, where significant improvement has to be made to lower energy consumption.

In the remineralization scheme Fig. 1, part of the ammonium can end up in the RO concentrate. Contacting Ammonium with OH^- in the base compartment of the BMED process may result in forming dissolved ammonia which is undesirable. However, ammonium concentration in our source water is very low (0.18 mM), and part of it will be sorped by the cation exchange and hence will not reach the RO concentrate (BMED feed). Therefore, the resulting dissolved ammonia concentration in the BMED base compartment will be low and not expected to be of large risk.

The developed remineralization process uses anaerobic groundwater as source water, which has a relatively stable water composition over time, therefore, rapid changes in feed water quality are not expected. However, assuming the application of the remineralization process on another source water (e.g., surface water), then a proper design of the process automatization should be investigated to accommodate the changes in the feed water quality. For the cation exchange process, conservative regeneration time can be considered to avoid leakage (breakthrough of undesired components) or frequent feed and effluent sampling to adjust the regeneration cycle duration. Furthermore, the remineralization process will be operated in batch and sequential mode where buffers should be created to store the eluents made and absorb any potential variation expected in the source water. The bipolar membrane electrodialysis process (BMED) is affected by the RO concentrate salinity which can be checked by monitoring the conductivity. Producing the right concentration of the acid and base can be monitored via pH measurement.

The yield and purity of the recovered calcium at different elution profiles using HCl eluent made from commercially available HCl stock solution 37 % (w/w) and produced HCl solution using BMED at the same concentration (0.81 M) were compared (Fig. 8). In both cases, linear gradient elution enhanced recovered calcium purity at the same yield. At 50 % yield (maximum purity achieved), recovered calcium purity using commercial HCl solution was almost the same (>99.0 %) for the different elution profiles tested. However, when the BMED-produced HCl was used in the CEX elution process, the recovered calcium purity was improved considerably at 50 % yield by applying linear and stepwise gradient elution profiles compared to an isocratic elution from 62.70 % to 84.0 %, respectively. This can be attributed to the lower purity of the BMED-produced HCl compared to the original HCl solution. In the BMED process, sodium can leak to the acid compartment due to imperfect selectivity of the anion exchange membrane, resulting in a less pure HCl solution. The purity of the BMED-produced HCl was >96 %. Fig. 8 Pareto front shows that using gradient elution a better separation between monovalent (sodium and potassium) and divalent ions (calcium) can be achieved even though the elution solution can be of lower purity.

3.4.2. Remineralization process cost estimate

The estimated cost of post-treating 1 m^3 of RO permeate using the developed remineralization process was calculated to explore the process economic feasibility. Table 3 shows the operational (OPEX) and capital (CAPEX) costs of the ion exchange resin and BMED units. The CAPEX included the resin material, ion exchange membranes, stack cost and peripheral equipment. While the OPEX included the chemicals, maintenance, and energy. The cost estimate is based on a mass balance calculation for a plant production capacity of 100 m^3/h at 95 % RO recovery using fresh groundwater at Oasen drinking water company treatment plant in Kamerik, the Netherlands. The groundwater characteristics are shown in Table S1 in the supplementary data. Extra NaCl was added to the feed to get around 1 M NaCl in the RO concentrate as feed for BMED to produce 1 M HCl and NaOH. The mass balance calculation aimed at achieving 1 mM of total hardness in the drinking water. The BMED process cost to produce 1 m^3 of 1 M HCl and NaOH was first calculated based on an earlier BMED process economic feasibility study by Strathmann and Koops [45]. Later, the BMED cost was converted based on the amount of chemicals needed in the CEX and AEX processes/m^3 water treated.

The total cost (CAPEX and OPEX) of the novel remineralization process is around 0.48 €/m^3 of water produced. That is higher than the conventionally applied remineralization processes using calcite filters (circa 0.1 €/m^3) [46]. It is also higher than other reported remineralization processes that focus on recovering hardness ions from source

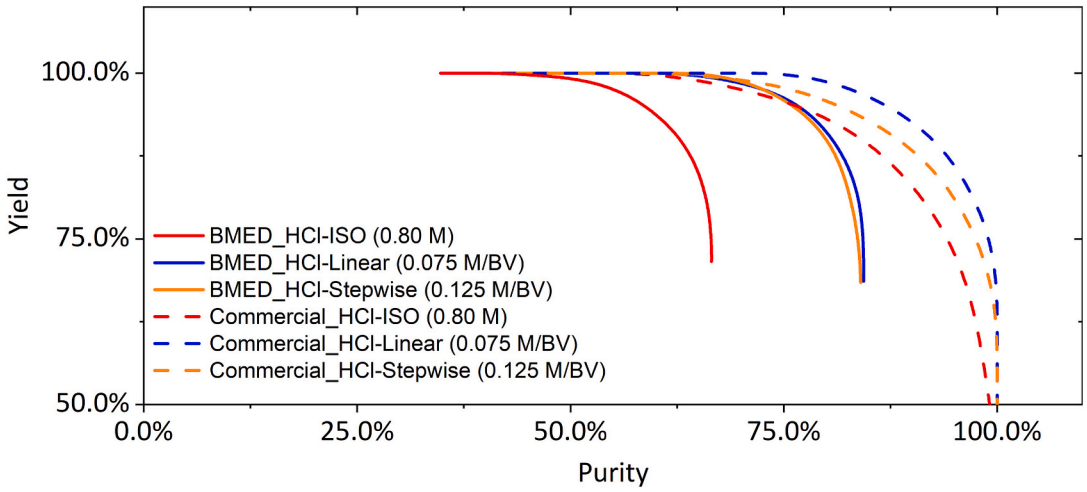

Fig. 8. The yield and purity curve of the separated calcium fraction using various elution profiles (isocratic, linear gradient and stepwise gradient) using commercially and BMED produced HCl acid. [HCl] = 0.81 M, room temperature ~ 22 °C. BV = bed volume.

Table 3
Cost analysis for the developed RO remineralization process using ion exchange resin and bipolar membrane electrodialysis.

Parameter		Unit	CEX	AEX	BMED
CAPEX[a]		€/m^3	0.03	0.03	0.15
OPEX	Chemicals[b]	€/m^3	–	0.03	–
	Maintenance[c]		0.01	0.01	0.04
	Energy[d]		0.003	0.003	0.18
Total		€/m^3	0.04	0.07	0.37

[a] Resin cost = 5 €/kg, ion exchange membrane cost = 235 €/m^2, bipolar membrane cost = 600 €/m^2.
[b] CO_2 cost is 100 €/ton.
[c] Maintenance is 10 % of the investment cost.
[d] Energy cost = 0.07 €/kWh, BMED current density = 750 A/m^2.

water [20]. The cost difference is largely due to the high production cost of the acid and base chemicals using BMED. BMED CAPEX was high due to the high membrane cost/m^2. Furthermore, BMED OPEX was high due to high energy requirements. Therefore, the BMED process is the limiting factor in the feasibility of the proposed remineralization process, and hence significant improvement has to be applied to BMED to reduce the total energy requirement and membrane cost.

However, by applying the developed on-site remineralization process, RO recovery can be increased to >95 % (in theory) due to the absence of scale-limiting divalent ions in the RO feed water. If ion exchange is not used in RO pre-treatment, then the RO recovery would be limited to 80 %. By taking the recovery improvement into account, the saving into RO CAPEX and OPEX was calculated (Supplementary data, part 2). When increasing the RO recovery from 80 % to 95 %, less modules and energy are needed. This results in roughly 0.2 €/m^3 saving in total treatment plant cost. This should compensate for the high cost of the remineralization process in comparison with conventional calcite remineralization at low recovery (80 %). Therefore, the developed remineralization process should be in an order of magnitude in comparison with other conventional RO remineralization processes.

4. Conclusion

This research presents a novel hybrid RO permeate remineralization process using a combination of bipolar membrane electrodialysis and ion exchange resin processes. The new remineralization process is advantageous to conventional ones in having less extra chemical use and CO_2 footprint. RO permeate remineralization is necessary to meet legal and guideline drinking water requirements and to protect the water distribution network by increasing the water buffering capacity. The limitations and efficiency of each of the processes forming the remineralization process were investigated. The CEX process hydrodynamics and ion exchange column efficiency were studied, furthermore, the effect of AEX feed water pH on potential calcium carbonate precipitate formation was tested. In addition, the production of high concentrations of HCl and NaOH from NaCl using BMED was tested. Moreover, the interplay and trade-off between the different components forming the developed remineralization process were analyzed. Finally, a cost analysis of the complete remineralization was done showing the process expected CAPEX and OPEX.

For the cation exchange process, the CEX process efficiency and breakthrough sharpness were significantly improved under low solution concentration and flow rate loading conditions. Frequent regeneration might be needed at higher loading flow rates and less sharper breakthrough curves. The yield and purity of the separated divalent ions were improved substantially by applying non-conventional gradient elution profiles. Hence, just by manipulating the elution profiles shape at the same eluent quantity, the purity and yield of the recovered fraction can be improved significantly.

For the anion exchange process, feed solution pH was found to be a significant factor in the AIX process efficiency and in preventing calcium precipitate during the calcium chloride/calcium bicarbonate exchange. Operating the AEX process under acidic conditions (pH < 2) is necessary to prevent calcium carbonate precipitate formation. However, bicarbonate yield during the AEX loading step was <50 % which implies the potential formation of carbonic acid and/or CO_2 bubbles. Therefore, the AEX process should be optimized, in terms of feed pH or way of operation to facilitate the removal of potentially formed CO_2 bubbles.

For the bipolar membrane electrodialysis process, the acid and base purity drop significantly with increasing the NaCl concentration in the feed solution due to the decrease in ion exchange membrane selectivity. HCl purity was >97 % at BMED feed solution concentration lower than 1.0 M. The use of a higher feed concentration at 3.0 M lowered the HCl purity by 10 %. Furthermore, BMED energy consumption is embedded in the stack operation i.e., membrane selectivity and applied current density.

The interplay and tradeoff between the elements forming the developed remineralization process were studied. BMED-produced HCl was successfully used in recovering calcium from the CEX resin at a similar purity and yield when commercial HCl is applied. In accordance with the criteria defined, the combination of bipolar membrane electrodialysis and ion exchange resin processes was proved to be feasible for remineralizing RO product water. The remineralization process

resulted in sufficient hardness concentration (1.0 mM Dutch standards) with high purity and yield. Yet, the efficient application of the presented remineralization process can be limited by water source characteristics (high feed water salinity is better), energy demand (highly selective IEX membranes are needed) and operational conditions. The total cost (CAPEX and OPEX) of the novel remineralization process was ~3 times (~0.48 €/m^3) higher than conventional processes. However, taking into account the total cost of the RO treatment process with the potential operation of the RO at 95 % recovery compared to 80 % when divalent ions are present, the total RO treatment cost is then comparable to conventional remineralization processes.

CRediT authorship contribution statement

A.A.M. Abusultan: Conceptualization, Formal analysis, Investigation, Methodology, Writing – original draft. **J.A. Wood:** Supervision, Writing – review & editing. **T. Sainio:** Writing – review & editing. **A.J.B. Kemperman:** Supervision, Writing – review & editing. **W.G.J. van der Meer:** Supervision, Writing – review & editing.

Declaration of competing interest

The authors declare the following financial interests/personal relationships which may be considered as potential competing interests: Almohanad Abusultan reports financial support was provided by Oasen NV. Walter van der Meer reports a relationship with Oasen NV that includes board membership and employment. Walter van der Meer, Almohanad Abusultan has a patent Method For Purifying Water As Well As Plant Suitable For Said Method issued to Oasen NV.

Data availability

Data will be made available on request.

Acknowledgement

This work was financially supported by Dutch water supply company OASEN N.V.

Appendix A. Supplementary data

Supplementary data to this article can be found online at https://doi.org/10.1016/j.desal.2023.117209.

References

[1] World Health Organization, UNICEF, Progress on drinking water, sanitation and hygiene 2000–2017: special focus on inequalities, New York, USA. Available online, https://www.unicef.org/reports/progress-on-drinking-water-sanitation-and-hygiene-2019, 2019 (accessed, 25 July 2022).
[2] Desal Data, Available online: www.DesalData.com, 2020. accessed on 25 July 2022.
[3] Ebrahimzadeh, S., Wols, B., Azzellino, A., Martijn, B.J., and van der Hoek, J.P., Quantification and modelling of organic micropollutant removal by reverse osmosis (RO) drinking water treatment. J. Water Process Eng., 2. 42. doi:https://doi.org/10.1016/j.jwpe.2021.102164.
[4] A. Egea-Corbacho Lopera, S. Gutiérrez Ruiz, J.M. Quiroga Alonso, Removal of emerging contaminants from wastewater using reverse osmosis for its subsequent reuse: pilot plant, J. Water Process. Eng. (2019) 29, https://doi.org/10.1016/j.jwpe.2019.100800.
[5] M. Sousi, Assessing Biological Stability of Drinking Water Produced by Reverse Osmosis and Remineralisation: Method Development and Application, University of Twente, 2021, https://doi.org/10.3990/1.9789036553018.
[6] J.C. Crittenden, R.R. Trussell, D.W. Hand, K. Howe, G. Tchobanoglous, MWH's Water Treatment: Principles and Design, Wiley, Hoboken, New Jersey, 2012, https://doi.org/10.1002/9781118131473.
[7] L.F. Greenlee, D.F. Lawler, B.D. Freeman, B. Marrot, P. Moulin, Reverse osmosis desalination: water sources, technology, and today's challenges, Water Res. 43 (9) (2009) 2317–2348, https://doi.org/10.1016/j.watres.2009.03.010.
[8] A. Antony, J.H. Low, S. Gray, A.E. Childress, P. Le-Clech, G. Leslie, Scale formation and control in high pressure membrane water treatment systems: a review, J. Membr. Sci. 383 (1) (2011) 1–16, https://doi.org/10.1016/j.memsci.2011.08.054.
[9] Y. Zhai, G. Liu, W.G.J. van der Meer, One-step reverse osmosis based on riverbank filtration for future drinking water purification, Engineering 9 (2022) 27–34, https://doi.org/10.1016/j.eng.2021.02.015.
[10] Drinkwaterbesluit, Available online: https://wetten.overheid.nl/BWBR0030111/2021-10-13 (accessed 20-10-2021).
[11] J. Liang, A. Deng, R. Xie, M. Gomez, J. Hu, J. Zhang, C.N. Ong, A. Adin, Impact of seawater reverse osmosis (SWRO) product remineralization on the corrosion rate of water distribution pipeline materials, Desalination 311 (2013) 54–61, https://doi.org/10.1016/j.desal.2012.11.010.
[12] N. Delion, G. Mauguin, P. Corsin, Importance and impact of post treatments on design and operation of SWRO plants, Desalination 165 (2004) 323–334, https://doi.org/10.1016/j.desal.2004.06.037.
[13] A. Withers, Options for recarbonation, remineralisation and disinfection for desalination plants, Desalination 179 (1) (2005) 11–24, https://doi.org/10.1016/j.desal.2004.11.051.
[14] N. Avni, M. Eben-Chaime, G. Oron, Optimizing desalinated sea water blending with other sources to meet magnesium requirements for potable and irrigation waters, Water Res. 47 (7) (2013) 2164–2176, https://doi.org/10.1016/j.watres.2013.01.018.
[15] D. Hasson, O. Bendrihem, Modeling remineralization of desalinated water by limestone dissolution, Desalination 190 (1) (2006) 189–200, https://doi.org/10.1016/j.desal.2005.09.003.
[16] R.D. Letterman, M. Hadad, C.T. Driscoll, Limestone contactors: steady-state design relationships, J. Environ. Eng. 117 (3) (1991) 339–358, https://doi.org/10.1061/(ASCE)0733-9372(1991)117:3(339).
[17] P. Nativ, N. Fridman-Bishop, O. Nir, O. Lahav, Dia-nanofiltration-electrodialysis hybrid process for selective removal of monovalent ions from Mg^{2+} rich brines, Desalination (2020) 481, https://doi.org/10.1016/j.desal.2020.114357.
[18] L. Birnhack, S.C.N. Tang, O. Lahav, Implementation, design and cost assessment of a membrane-based process for selectively enriching desalinated water with divalent seawater ions, ChemEngineering 2 (3) (2018), https://doi.org/10.3390/chemengineering2030041.
[19] M. Philibert, A. Filingeri, C. Natalelloa, N. Moe, E. Filloux, A. Cipollina, Surface water RO permeate remineralization through minerals recovery from brines, Desalination (2022) 531, https://doi.org/10.1016/j.desal.2022.115725.
[20] A. Lesimple, F.E. Ahmed, N. Hilal, Remineralization of desalinated water: methods and environmental impact, Desalination (2020) 496, https://doi.org/10.1016/j.desal.2020.114692.
[21] A. Lesimple, F.E. Ahmed, N. Hilal, Remineralization of desalinated water: methods and environmental impact, Desalination 496 (2020), 114692, https://doi.org/10.1016/j.desal.2020.114692.
[22] Van der Meer, W.G.J. and Abusultan, A.A.M., Method for purifying water as well as plant suitable for said method. 2018. Patent application number: EP 18161272. Available online: https://patentscope.wipo.int/search/en/detail.jsf?docId=EP226147242 (accessed 14-08-2023).
[23] WHO Guidelines Approved by the Guidelines Review Committee, Guidelines for Drinking-water Quality: Fourth Edition Incorporating the First and Second Addenda, World Health Organization, Geneva, 2022. Available online: https://www.who.int/publications/i/item/9789240045064 (accessed 14-08-2023).
[24] A.A.M. Abusultan, J.A. Wood, T. Sainio, A.J.B. Kemperman, W.G.J. van der Meer, Ion exchange resin — bipolar membrane electrodialysis hybrid process for reverse osmosis permeate remineralization: cation exchange resins equilibria and kinetics, Sep. Purif. Technol. (2023), https://doi.org/10.1016/j.seppur.2023.123798.
[25] A.A.M. Abusultan, J.A. Wood, T. Sainio, A.J.B. Kemperman, W.G.J. van der Meer, Ion exchange resin — bipolar membrane electrodialysis hybrid process for reverse osmosis permeate remineralization: preparative ion exchange chromatography for Ca^{2+} and Mg^{2+} recovery, Sep. Purif. Technol. (2023), https://doi.org/10.1016/j.seppur.2023.123799.
[26] K.H. Gebauer, J. Thömmes, M.R. Kula, Breakthrough performance of high-capacity membrane adsorbers in protein chromatography, Chem. Eng. Sci. 52 (3) (1997) 405–419, https://doi.org/10.1016/S0009-2509(96)00426-5.
[27] T. Vermeulen, N.K. Hiester, Ion-exchange and adsorption column kinetics with uniform partial presaturation, J. Chem. Phys. 22 (1) (1954) 96–101, https://doi.org/10.1063/1.1739865.
[28] R. Pärnamäe, S. Mareev, V. Nikonenko, S. Melnikov, N. Sheldeshov, V. Zabolotskii, H.V.M. Hamelers, M. Tedesco, Bipolar membranes: a review on principles, latest developments, and applications, J. Membr. Sci. (2021) 617, https://doi.org/10.1016/j.memsci.2020.118538.
[29] A.A.M. Abusultan, J.A. Wood, A.J.B. Kemperman, W.G.J. van der Meer, Valorisation of HCl and NaOH from softened reverse osmosis concentrate using bipolar membrane electrodialysis, To be submitted to, Water Sci. Technol. J. (2023).
[30] J.J. Van Deemter, F.J. Zuiderweg, A. Klinkenberg, Longitudinal diffusion and resistance to mass transfer as causes of nonideality in chromatography, Chem. Eng. Sci. 5 (6) (1956) 271–289, https://doi.org/10.1016/0009-2509(56)80003-1.
[31] E. Glueckauf, Theory of chromatography. Part 9. The "theoretical plate" concept in column separations, Trans. Faraday Soc. 51 (0) (1955) 34–44, https://doi.org/10.1039/TF9555100034.
[32] A.J. Martin, R.L. Synge, A new form of chromatogram employing two liquid phases: a theory of chromatography. 2. Application to the micro-determination of the higher monoamino-acids in proteins, Biochem. J. 35 (12) (1941) 1358–1368, https://doi.org/10.1042/2Fbj0351358.
[33] G. Guiochon, D.G.G. Shirazi, A. Felinger, A.M. Katti, Fundamentals of Preparative and Nonlinear Chromatography, Elsevier Science, United States, 2006.

[34] A.L. Myers, S. Byington, Thermodynamics of ion exchange: prediction of multicomponent equilibria from binary data, in: A.E. Rodrigues (Ed.), Ion Exchange: Science and Technology, Springer Netherlands, Dordrecht, 1986, pp. 119–145, https://doi.org/10.1007/978-94-009-4376-6_5.
[35] F.G. Helfferich, Ion Exchange, Dover, 1995.
[36] Y. Shan, A. Seidel-Morgenstern, Optimization of gradient elution conditions in multicomponent preparative liquid chromatography, J. Chromatogr. A 1093 (1) (2005) 47–58, https://doi.org/10.1016/j.chroma.2005.07.047.
[37] A. Felinger, G. Guiochon, Comparing the optimum performance of the different modes of preparative liquid chromatography, J. Chromatogr. A 796 (1) (1998) 59–74, https://doi.org/10.1016/s0021-9673(97)01075-3.
[38] W.M. Haynes, CRC Handbook of Chemistry and Physics, 97th ed., CRC Press, United states, 2016 https://doi.org/10.1201/9781315380476.
[39] C.B. Andersen, Understanding carbonate equilibria by measuring alkalinity in experimental and natural systems, J. Geosci. Educ. 50 (4) (2002) 389–403, https://doi.org/10.5408/1089-9995-50.4.389.
[40] Chapter 1 The CO_2-carbonic acid system and solution chemistry, in: J.W. Morse, F. T. Mackenzie (Eds.), Developments in Sedimentology, Elsevier, 1990, pp. 1–38, https://doi.org/10.1016/S0070-4571(08)70330-3.
[41] FUMATECH-BWT-GmbH, Fumasep FKB-PK-130 and FAB-PK-130 Membrane Technical Datasheet, 2020.
[42] H. Strathmann, Ion-exchange Membrane Separation Processes, Elsevier Science, Amsterdam, The Netherlands, 2004.
[43] Guidelines for Drinking-Water Quality: Fourth Edition Incorporating the First Addendum, World Health Organization, Geneva, 2017.
[44] V.G. Gude, Energy consumption and recovery in reverse osmosis, Desalin. Water Treat. 36 (1–3) (2011) 239–260, https://doi.org/10.5004/dwt.2011.2534.
[45] H. Strathmann, G. Koops, Process economics of electrodialytic water dissociation for the production of acid and base, in: Handbook on Bipolar Membrane Technology, 2000, pp. 191–220.
[46] O. Lehmann, L. Birnhack, O. Lahav, Design aspects of calcite-dissolution reactors applied for post treatment of desalinated water, Desalination 314 (2013) 1–9, https://doi.org/10.1016/j.desal.2012.12.017.